Photostability of luminescence of Ag$_2$S quantum dots and Ag$_2$S/SiO$_2$ core/shell structures

© I.G. Grevtseva, O.V. Ovchinnikov, M.S. Smirnov, T.S. Kondratenko, V.N. Derepko, A.M.Kh. Hussein, N.E. Egorov, E.A. Vozgorkova

Voronezh State University,
394018 Voronezh, Russia

e-mail: grevtseva_ig@inbox.ru

The paper presents regularities that demonstrate the effect of passivating ligands formation of thioglycolic acid and L-cysteine (TGA, L-Cys) and dielectric shells (SiO$_2$) on Ag$_2$S nanocrystals interface on the photostability of their IR luminescence. Using FTIR absorption spectroscopy, the interaction manifestations of passivating ligands molecules of TGA and L-Cys with Ag$_2$S nanocrystals, as well as the formation of SiO$_2$ shell due to the process of replacing organic ligands with a silica ligand (MPTMS) („ligand exchange"), were found. In the case of replacing TGA with MPTMS, an increase in the luminescence quantum yield of Ag$_2$S quantum dots (QDs) and its resistance to long-term exposure to exciting radiation was found. In the case of replacing L-Cys with MPTMS, the formation of a fragmentary SiO$_2$/L-Cys shell on Ag$_2$S nanocrystals was observed due to the partial replacement of L-Cys with MPTMS, which contributes to the reverse photodegradation of KT Ag$_2$S luminescence of as a result of SiO$_2$/L-Cys shell photodestruction.

Keywords: photoluminescence, luminescence photostability, quantum yield, quantum dot, core/shell structures, FTIR spectroscopy.

DOI: 10.21883/EOS.2022.12.55254.4106-22

Introduction

Semiconductor colloidal quantum dots (QDs), which are semiconductor nanocrystals coated with organic passivator molecules or shells of wide-band inorganic semiconductors or dielectrics, are promising materials for a variety of photonics devices. These include radiation detectors, emitters, photocatalytic and sensor systems, luminescent markers [1–10]. One of the fundamental problems that arise in the way of the applied use of QDs in applications based on luminescence is its degradation under the action of photoexciting quanta [11–37]. A significant influence of the non-stoichiometry of the compound from which QDs [11–18] were synthesized was noted. Photodegradation of IR luminescence has been repeatedly observed in colloidal Ag$_2$S QDs, the composition of which has a high degree of non-stoichiometry [21–28]. At the same time, the influence of the surface environment (solvent, passivating ligands, stabilizing polymers, organic dye molecules, etc.) on the luminescence parameters of QDs was found [21–27]. However, the role of photochemical processes both in the nanocrystals themselves and with the participation of molecules of the surface environment remains virtually unexplained, which significantly complicates the optimization of synthesis conditions that ensure the preservation of the luminescent parameters of QDs during photoexcitation.

A separate scientific and practical interest is the solution of the problem of controlling the luminescent properties of QDs by modifying the surface of colloidal QDs by forming a shell of wide-band semiconductors (core/shell structure) [28–38]. For core/shell structures, the issue of luminescence stability is also of significant importance. Despite the increase in the quantum yield of luminescence during the formation of hydrophilic core/shell structures, prolonged exposure to exciting radiation leads to photodegradation of their luminescent properties [28–38]. Similar patterns were observed for QDs of CdSe/ZnS, CdSe/CDs, CdSeZnS/ZnS, Ag$_2$S/ZnS, etc. At the same time, the causes and mechanisms of the processes underlying photodegradation of luminescence of colloidal QDs core/shell, as a rule, are not discussed in detail. The authors of [29] suggest that an effective way to quench CdSe/ZnS QDs luminescence is the transfer of excited charge carriers from the QDs core to surface ligands or surrounding molecules, due to the mutual arrangement of the energy levels of the Highest energy Occupied Molecular Orbital (HOMO) — Lowest energy Unoccupied Molecular Orbital (LUMO) of surface ligands and CdSe/ZnS QDs. In the work [30] it is shown that the greatest photostability of luminescence of CdSe/ZnS nanocrystals is provided by the strong bond of amphiphilic polymers with their surface due to the high degree of hydrophobicity of QDs packaging in the polymer. Cross-links in the polymer structure make it difficult for oxygen to diffuse to the surface of the nanocrystal, thereby preventing photo-oxidation of the ZnS shell and reducing the photostability of luminescence. The authors of the work [32,33] came to similar conclusions. They showed that activation of photoinduced CdSe/ZnS

processes does not occur in vacuum conditions. At the same time, the luminescence efficiency decreases in air due to the predominance of photooxidation over the passivation of surface defects by the ZnS shell, which increases the probability of non-radiative transitions and reduces the luminescence intensity.

Thus, the question of the influence of the formation of shells and their thickness on the photostability of QDs luminescence, as well as the identification of the main causes of its photodegradation, remains relevant.

This work is devoted to the establishment of empirical regularities of photostability of the luminescence of QDs core/shell Ag$_2$S/SiO$_2$, formed under conditions of various mechanisms of passivation of the surface of Ag$_2$S QDs molecules of thiol-containing acids (thioglycolic acid (TGA) and L-cysteine (L-Cys)).

Materials and Measurement Techniques

Samples of colloidal Ag$_2$S QDs, passivated with TGA and L-Cys molecules (hereinafter Ag$_2$S/TGA QDs and Ag$_2$S/L-Cys QDs) were obtained within the framework of an aqueous colloidal synthesis. The synthesis of colloidal Ag$_2$S/TGA QDs consisted in mixing aqueous solutions of two precursors. The first is a mixture of aqueous solutions of AgNO$_3$ and TGA in a molar ratio of 1 : 1 at pH 10, and the second is an aqueous solution of Na$_2$S, the concentration of which corresponded to the molar ratio [AgNO$_3$] : [TGA] : [Na$_2$S], equal to 1 : 1 : 0.33. The colloidal solution was kept 24 h at a temperature of 25°C and constant stirring (300 rot/min) [21–24]. The synthesis of colloidal Ag$_2$S/L-Cys QDs was carried out by mixing aqueous solutions of AgNO$_3$ and L-Cys in a molar ratio equal to 1 : 2, followed by bringing the pH value to 10. Next, the colloidal mixture was kept 1.5 h at a temperature of 90°C and constant stirring (300 rot /min) [25]. To remove by-products of the reaction, colloidal Ag$_2$S/TGA QDs and Ag$_2$S/L-Cys QDs were centrifuged with the addition of acetone in the ratio 1 : 1.

The formation of the core/shell Ag$_2$S/SiO$_2$ QDs, and the control of the thickness of the dielectric shell SiO$_2$ on the QDs surface Ag$_2$S in the framework of the aqueous synthesis technique is based on the use of silica ligand 3-mercaptopropyl trimethoxysilane (MPTMS) as a binding agent and sodium metasilicate (Na$_2$SiO$_3$) as a precursor of the SiO$_2$ base layer [38]. The concentration of the introduced MPTMS solution in each case was calculated based on the concentration and average size of QDs in the ensemble and was for Ag$_2$S/TGA QDs — 8 mM (hereinafter Ag$_2$S(TGA)/MPTMS QDs), and for Ag$_2$S/L-Cys QDs — 4 mM (hereinafter Ag$_2$S(L-Cys)/MPTMS QDs). Thus, at this stage, 1−2 layers of SiO are formed on the surface of the Ag$_2$S$_2$ QDs ($\sim$ 0.7−1.5 nm, according to the MPTMS molecule size data [39]). Further, an aqueous solution of Na$_2$SiO$_3$ was introduced into the reaction mixture. Depending on the applied concentration of Na$_2$SiO$_3$ into

the reaction mixture (10−70 mM) the thickness of the SiO$_2$ layer on the QDs surface varied (hereinafter referred to as QDs Ag$_2$S(TGA)/SiO$_2$ QDs, and Ag$_2$S(L-Cys)/SiO$_2$) QDs, reaction time is 24 h.

As a model sample of QDs core/shell, a sample was synthesized for which the silica ligand MPTMS served simultaneously as a passivating ligand and a precursor of the SiO$_2$ shell. This approach allows the formation of core/shell structures based on Ag$_2$S QDs without the use of thiocarboxylic acid molecules (hereinafter Ag$_2$S/SiO$_2$ QDs). The method of synthesis of Ag$_2$S/SiO$_2$ QDs consisted in mixing aqueous solutions of AgNO$_3$ and MPTMS in a molar ratio of 1 : 2 at pH 10 and subsequent introduction into the reaction mixture of an aqueous solution of Na$_2$S, the concentration of which corresponded to the molar ratio [AgNO$_3$] : [MPTMS] : [Na$_2$S] as 1 : 2 : 0.6.

The Sigma-Aldrich chemical reagents used in the work had a High Purity degree.

The size of the core/shell structures based on Ag$_2$S QDs was determined using a transmission electron microscope (TEM) Libra 120 (CarlZeiss, Germany). Data on the crystal structure of QDs were obtained using high-resolution TEM — JEOL 2000FX (JEOLLtd., Japan).

The absorption properties were studied using a USB2000+ spectrometer (Ocean Optics, USA) with a USB-DT continuous radiation source (Ocean Optics, USA). The luminescence spectra were recorded using a spectral complex based on the MDR-4 diffraction monochromator (LOMO, Russia) with a near-IR photodetector — PDF10C/M photodiode (ThorlabsInc., USA). The photostability of the luminescent properties of the core/shell structures based on Ag$_2$S QDs was evaluated by monitoring the intensity of luminescence at the peak of luminescence over time of exposure to radiation. Photoluminescence excitation was carried out by laser diodes LD PLTB450 (Osram, Germany) with a wavelength of 445 nm and an optical power of 400 mW and LPC-836 (Mitsubishi Electric, Japan) with a wavelength of 660 nm and an optical power of 250 mW.

IR absorption spectra were recorded using an FTIR spectrometer Tensor 37 (Bruker Optik GmbH, Germany). To study the IR absorption spectra, colloidal QDs solutions were applied to KCl substrates and free water was removed by evaporation in a drying cabinet at a temperature of 60°C. The solutions deposited on the KCl substrate had equal volumes.

Results and discussion

Structural characteristics of the studied samples

Data on structural properties, sizes, morphology and crystal structure were obtained for all synthesized samples. First of all, studies performed on the Libra-120 transmission electron microscope TEM showed the formation in these cases of ensembles of individual Ag$_2$S/TGA QDs with a size of 2.5 $\pm$ 0.5 nm and a dispersion of 20% (Fig. 1, *a*), as
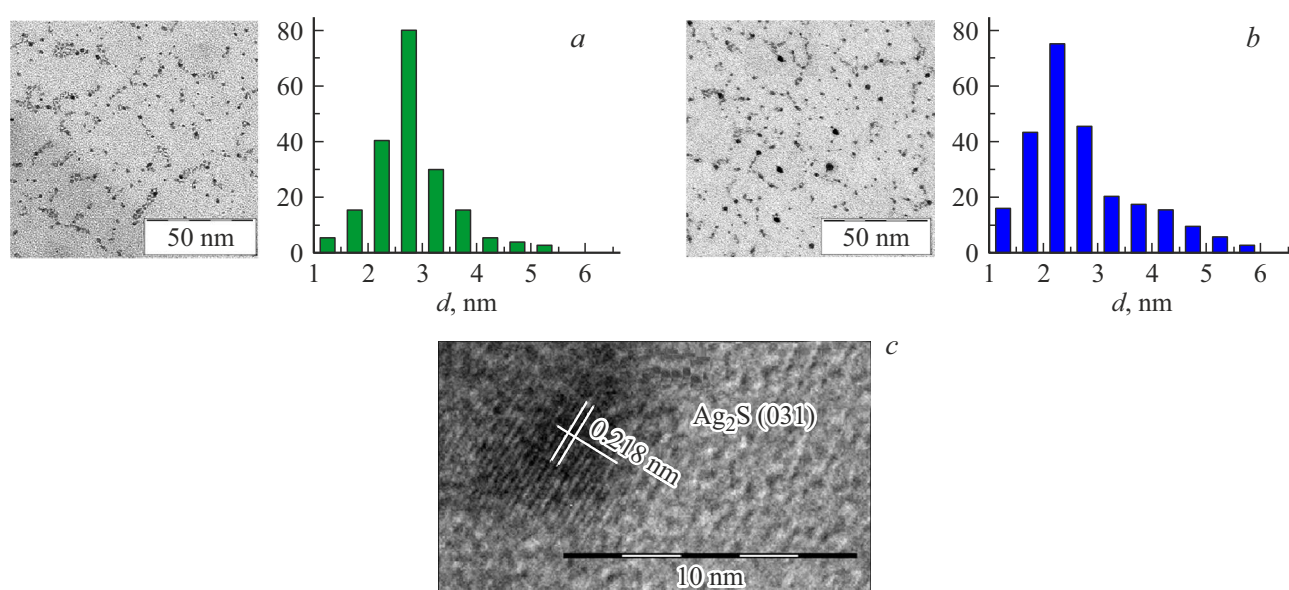
Figure 1. TEM images and histograms of the size distribution of ensembles Ag_2S/TGA QDs (*a*) and Ag_2S/L-Cys QDs (*b*). High-resolution TEM image QDs Ag_2S/TGA (QDs Ag_2S/L-Cys) (*c*).

well as Ag_2S/L-Cys QDs — 2.5 ± 0.7 nm, dispersion of 30% (Fig. 1, *b*).

High-resolution TEM images of synthesized samples showed electron diffraction mainly from the crystallographic plane (031), indicating the formation of nanocrystals with interatomic distances of 0.218 nm (Fig. 1, *with*). Thus, using the high-resolution TEM method for all the above samples, it was found that the Ag_2S QDs are formed in a monoclinic lattice (spatial group P21/c).

Formation of structures core/shell QDs of $Ag_2S(TGA)/SiO_2$, $Ag_2S(L$-Cys$)/SiO_2$ and Ag_2S/SiO_2 is confirmed by comparing dark-field and light-field TEM images from the same fragment of the substrate (Fig. 2, *a, b, c*).

Intense electron diffraction from Ag_2S QDs was observed on dark-field images. At the same time, the image from the amorphous dielectric SiO_2 was low-contrast. Thus, the obtained differences in the size of $Ag_2S(TGA)/SiO_2$ QDs at the maximum concentration of Na_2SiO_3 on dark-field ($2.8 - 0.5$ nm) and light-field images (10.2 ± 2.5 nm) are caused by the formation of an amorphous shell SiO_2 with a thickness of $\sim 3.5 \pm 1.2$ nm (Fig. 2, *a*). For $Ag_2S(L$-Cys$)/SiO_2$ QDs differences in size at the maximum concentration of Na_2SiO_3 on dark-field (3.0 ± 0.5 nm) and light-field images (5.5 ± 1.5 nm) are attributed to the formation of the shell SiO_2 thick $\sim 2.5 \pm 0.5$ nm (Fig. 2, *b*). We note that in some cases the formation of Ag_2S QDs agglomerates, were observed, covered with a common layer of SiO_2 up to 3 nm thick for $Ag_2S(TGA)/SiO_2$ QDs and up to 1.5 nm thick for $Ag_2S(L$-Cys$)/SiO_2$ QDs. In addition to the formation of the SiO_2 shell, a slight growth of Ag_2S nuclei was observed within 0.5 nm, due to the presence of active sulfur

in MPTMS. The dispersion in the size of the QDs in the ensemble reached 35%.

Analysis of TEM images of a Ag_2S/SiO_2 QDs model sample, for which the MPTMS silica ligand simultaneously served as a passivating ligand and a precursor of the SiO_2 shell, showed differences in size on dark-field (1.8 ± 0.5 nm) and light-field images (5.0 ± 1.5 nm), which is caused by the formation of the shell SiO_2 with a thickness of $\sim 1.6 \pm 0.8$ nm (Fig. 2, *with*) with a QDs size dispersion of about 30%.

Spectral-luminescent properties of the studied samples

During the formation of the Ag_2S QDs core/shell, some changes were observed in the optical absorption spectra (Fig. 3, *a, b*, inset). As a result of the formation of $Ag_2S(TGA)/MPTMS$ QDs structures, there was a slight change in the shape of the absorption spectrum — a weak increase in optical density in the region of 2.1 and 1.3 eV (Fig. 3, *a*, inset, curve *2*). The peculiarity in the area of 1.9 eV disappeared. Subsequent formation of $Ag_2S(TGA)/SiO_2$ QDs structures, resulted in an increase in optical density in the region of 1.3 eV. At the same time, a feature was formed in the region of 1.6 eV, and in the region of 1.9 eV, on the contrary, disappeared (Fig. 3, *a*, inset, curve *3*). The observed patterns are the result of a change in the size distribution of Ag_2S QDs in solution, as well as the formation of Ag_2S QDs agglomerates coated with a common layer of SiO_2, as a result of the addition of a sulfur-containing silica ligand MPTMS to the colloidal solution [38]. During the formation of $Ag_2S(L$-Cys$)/MPTMS$ QDs, an increase in optical density is observed over the entire spectrum with simultaneous
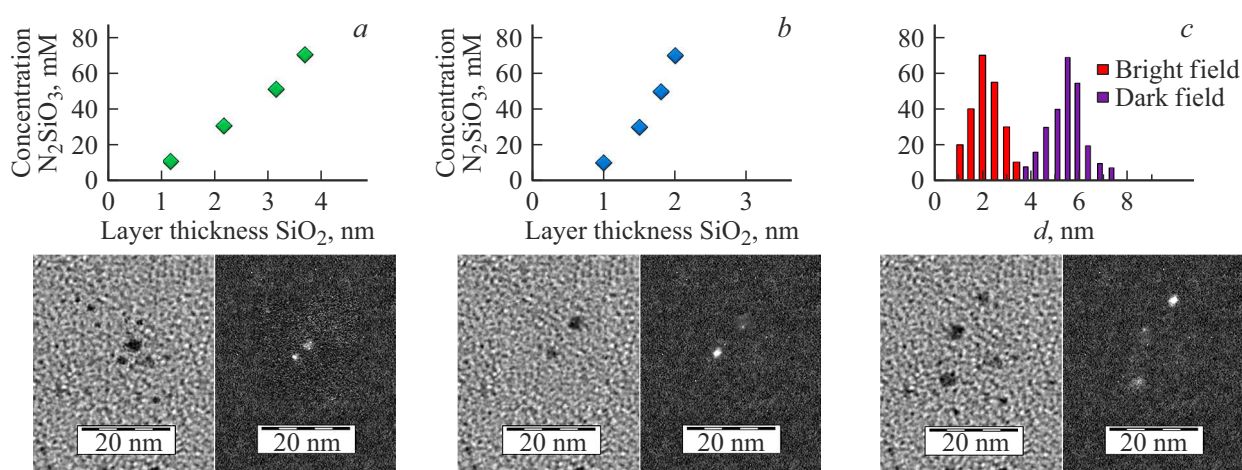
Figure 2. Light-field and dark-field TEM images (below) for Ag$_2$S/SiO$_2$/TGA QDs (*a*), Ag$_2$S/SiO$_2$/L-Cys QDs (*b*) and Ag$_2$S/SiO$_2$ QDs (*c*). Dependences of the thickness of the SiO$_2$ layer on the QDs surface on the concentration of Na$_2$SiO$_3$ (top) for Ag$_2$S/SiO$_2$/TGA QDs (*a*), Ag$_2$S/SiO$_2$/L-Cys QDs (*b*) and size distribution histogram (top) for Ag$_2$S/SiO$_2$ QDs (*c*).

blurring and displacement of the feature from 1.9 to 1.8 eV (Fig. 3, *b*, inset, curve *2*). An increase in the thickness of the layer SiO$_2$ on the QDs surface Ag$_2$S(L-Cys)/SiO$_2$ leads to the disappearance of a feature in the absorption spectrum (Fig. 3, *b*, inset, curve *3*). Such behavior of the absorption properties of Ag$_2$S(L-Cys)/MPTMS QDs and Ag$_2$S(L-Cys)/SiO$_2$ QDs is also the result of the growth of QDs and an increase in their size dispersion in the ensemble, which is consistent with the TEM data.

For the samples of QDs of Ag$_2$S/TGA, Ag$_2$S/L-Cys and Ag$_2$S/SiO$_2$, a luminescence band with a half-width of about 100 was observed,nm and peaks in the region of 960 and 750 nm, respectively. A significant Stokes shift of $\sim 0.3-0.5$ eV, indicates the trap-state luminescence nature in the IR region for these samples [21–23,25]. Previously, for the IR luminescence of colloidal Ag$_2$S QDs passivated with thiocarboxylic acids, it was found that the glow occurs as a result of recombination of electrons localized at the levels of interface defects with free holes [41].

It was found that for Ag$_2$S/L-Cys QDs and Ag$_2$S/SiO$_2$ QDs, similar to Ag$_2$S/TGA QDs,, the luminescence peak. It is located in the shorter wavelength region of the spectrum at 750 nm (Fig. 3). This behavior indicates the localization of trap-state luminescence centers near the interfaces of nanocrystals and the effect of the ligand type on the luminescent properties of Ag$_2$S QDs [41].

The peak of the luminescence spectrum of Ag$_2$S/TGA QDs (960 nm) during the formation of Ag$_2$S(TGA)/MPTMS QDs is shifted to the long-wavelength region to 992 nm. At the same time, the quantum yield of luminescence increases by 7 times (Fig. 3, *a*, curve *2*). The subsequent increase in the thickness of the SiO$_2$ layer at the Ag$_2$S/TGA QDs interfaces, contributes to a short-wave shift of the lumines-cence peak (950 nm) and an increase in the quantum yield by 35 times (Fig. 3, *a*, curve *2*). The formation of QDs structures of QDs structures of Ag$_2$S(LCys)/MPTMS, and

Ag$_2$S(L-Cys)/SiO$_2$ also contributes to the long-wavelength shift of the luminescence band from 750 to 820 nm and an increase in its quantum yield by 3 times (Fig. 3, *b*). The spectral shift of the luminescence peak during the formation of the SiO$_2$ shell and an increase in its thickness confirms the assumption of localization of the luminescence center near the QDs interfaces (Fig. 3, *a, b*, inset).

Photostability of luminescent properties of the studied samples

As the time of action of exciting radiation on the studied samples of ensembles of colloidal Ag$_2$S QDs increased, degradation of IR luminescence was observed in most cases (Fig. 4). Characteristic decay times of luminescence intensity for Ag$_2$S QDs under the action of radiation with a wavelength of 445 nm ($35 \cdot 10^{17}$ quant/cm^2·s) and 660 nm ($5 \cdot 10^{17}$ quant/cm^2·s), falling on the exciton absorption region of Ag$_2$S QDs, are $5-10$ min (fig. 4). It should be noted that the optical absorption spectra do not change after photofloworing. This indicates the absence of the influence of the photo-etched process of Ag$_2$S QDs.

The most noticeable process of photodegradation of luminescence was observed in the case of Ag$_2$S/TGA QDs with trap-state luminescence in the region of $870-1000$ nm, considered in this work. For this sample, the photodegra-dation process is reversible (Fig. 4, *a*, curve *1*). The luminescence intensity is restored when the sample is kept in the dark for 24 h. We note that in the case of Ag$_2$S/TGA QDs with excitonic luminescence with a peak at 620 nm, the degradation process did not exceed $10-15\%$ and turned out to be irreversible (Fig. 4, *a*, curve *2*). These patterns are completely consistent with similar studies [21–24].

Normalized dependences of luminescence intensity on the time of exposure to exciting radiation for ensembles of colloidal Ag$_2$S/L-Cys QDs showed its photostability (Fig. 4, *b*, curve *1*) similar to the data of [25].
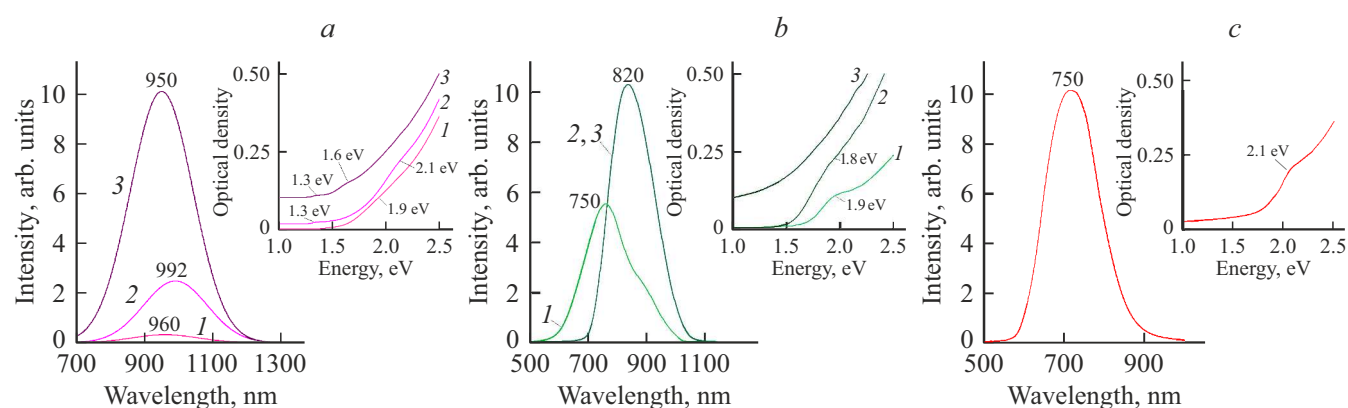
Figure 3. Optical absorption (inset) and luminescence spectra of Ag$_2$S/TGA QDs (*a*) and Ag$_2$S/L-Cys QDs (*b*), as well as core/shell structures based on them: Ag$_2$S/TGA QDs and Ag$_2$S/L-Cys QDs (*1*); Ag$_2$S(TGA)/MPTMS QDs and Ag$_2$S(L-Cys)/MPTMS QDs (*2*), Ag$_2$S(TGA)/SiO$_2$ QDs and Ag$_2$S(L-Cys)/SiO$_2$ QDs (*3*). Optical absorption (inset) and luminescence spectra of the core/shell structures of Ag$_2$S/SiO$_2$ QDs (*c*).

Luminescence parameters of Ag$_2$S QDs and core/shell structures based on them (the luminescence parameters after exposure are indicated in brackets)

Sample type	λ_{lum}, nm	QY, %	τ, ns	r_r, s^{-1}	r_{nr}, s^{-1}
Ag$_2$S/TGA QDs	960	0.1 (0.04)	3.5 (2.0)	$3 \cdot 10^5$ ($2 \cdot 10^5$)	$3 \cdot 10^8$ ($5 \cdot 10^8$)
Ag$_2$S/MPTMS/TGA QDs	992	0.7 (0.6)	7.7 (6.8)	$9 \cdot 10^5$ ($9 \cdot 10^5$)	10^8 (10^8)
Ag$_2$S/SiO$_2$/TGA QDs	950	3.5 (3.5)	17.7 (17.3)	$2 \cdot 10^6$ ($2 \cdot 10^6$)	$5 \cdot 10^7$ ($5 \cdot 10^7$)
Ag$_2$S/L-Cys QDs	750	0.3 (0.3)	7.2 (7.2)	$4 \cdot 10^5$ ($4 \cdot 10^5$)	10^8 (10^8)
Ag$_2$S/MPTMS/L-Cys QDs	820	0.7 (0.2)	9.4 (3.2)	$7 \cdot 10^5$ ($6 \cdot 10^5$)	10^8 ($3 \cdot 10^8$)
Ag$_2$S/SiO$_2$/L-Cys QDs	820	0.9 (0.01)	9.8 (2.1)	10^6 ($5 \cdot 10^4$)	10^7 ($5 \cdot 10^8$)
Ag$_2$S/SiO$_2$ QDs	750	1.0 (0.9)	4.0 (4.0)	$3 \cdot 10^6$ ($2 \cdot 10^6$)	$2 \cdot 10^8$ ($2 \cdot 10^8$)

The model sample of Ag$_2$S/SiO$_2$ QDs, for which the silica ligand MPTMS acted simultaneously as a passivating ligand and a precursor of the shell SiO$_2$, demonstrates stable luminescence under prolonged exposure to exciting radiation (Fig. 4, *with*).

The formation of the SiO$_2$ shell on the Ag$_2$S/TGA QDs, leads to blocking the degradation process of IR luminescence against the background of an increase in the quantum yield of luminescence (Table) as with a shell thickness of several monolayers of SiO$_2$ for Ag$_2$S(TGA)/MPTMS QDs, and in several nanometers for Ag$_2$S(TGA)/SiO$_2$ QDs (Fig. 4, *a*, curves *3, 4*). Moreover, in the latter case, the photostability of luminescence turned out to be higher than when covering SiO$_2$ with a shell of several monolayers.

The stability of luminescence intensity demonstrated for Ag$_2$S/L-Cys QDs to prolonged exposure to radiation of different power and wavelength (Fig. 4, *b*, curve *1*) [25] On the contrary, it was violated during the formation of the shell SiO$_2$. At the same time, the formation of the SiO$_2$ shell into several monolayers in the case of Ag$_2$S(L-Cys)/MPTMS QDs leads to degradation of IR luminescence

by 70−80% and even greater degradation of ∼ 95% when trying to increase the thickness of the shell by participating in the reaction Na$_2$SiO$_3$ (Ag$_2$S(L-Cys)/SiO$_2$ QDs) (Fig. 4, *b*, curves *2, 3*). it is established that photodegradation of the luminescence of Ag$_2$S(L-Cys)/MPTMS QDs and Ag$_2$S(L-Cys)/SiO$_2$ QDs is irreversible. Exposure after exposure to Ag$_2$S(L-Cys)/MPTMS QDs and Ag$_2$S(L-Cys)/SiO$_2$ QDs in the dark for 24 h does not lead to the recovery of intensity their luminescence.

Thus, the photostability of the luminescence of Ag$_2$S QDs, and core/shell structures based on them is determined not only by the type of passivating ligands, but also by the approach to the formation of core/shell structures. In addition, it is known that the state of the surface of micro- and nanocrystals (especially the concentration of adatoms and low-atom clusters) has a significant effect on the photostability of luminescence of various crystals, such as silver halides, zinc sulfides and cadmium [43–48]. This effect is called „luminescence fatigue" and is explained by photostimulated formation of metal clusters — channels of non-radiative recombination on the surface of crystals,
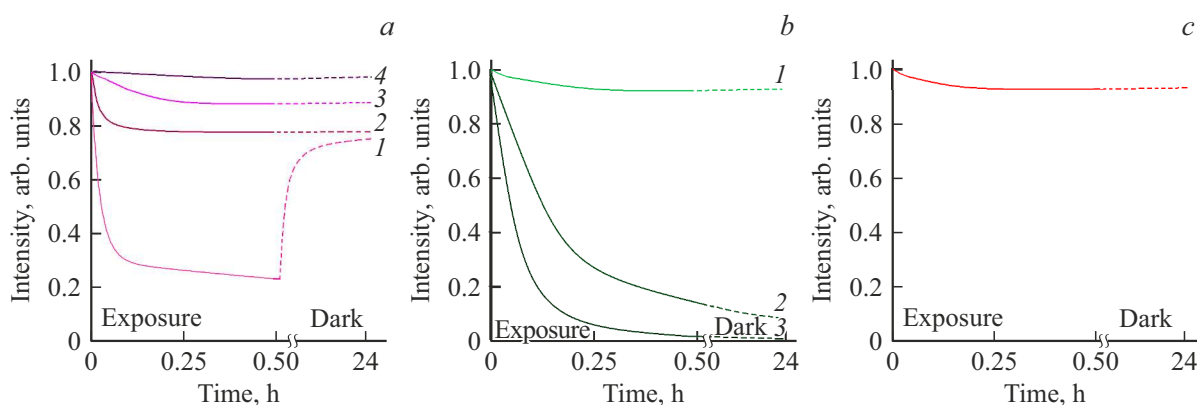
Figure 4. Normalized dependences of luminescence intensity on the time of exposure to exciting radiation for ensembles of colloidal Ag₂S/TGA QDs with trap-state luminescence in the region of 870−1000 nm (*1*), Ag₂S/TGA QDs with exciton luminescence at 620 nm (*2*), Ag₂S(TGA)/MPTMS QDs (*3*), Ag₂S(TGA)/SiO₂ QDs (*4*) — *a*. Normalized dependences of luminescence intensity on the time of exposure to exciting radiation for ensembles of colloidal Ag₂S/L-Cys QDs (*1*), Ag₂S(L-CyS)/MPTMS QDs (*2*), Ag₂S(L-Cys)/SiO₂ QDs (*3*) — *b*. Normalized dependences of luminescence intensity on the time of exposure to exciting radiation for ensembles of colloidal Ag₂S/SiO₂ QDs — *c*.

including due to the initial stage of photolysis developing on the surface. A similar conclusion was reached by the authors of [23] in the case of the formation of Ag₂S QDs in gelatin. The fact of photodegradation of luminescence intensity was also analyzed in the case of Ag₂S/TGA QDs, including photostability, depending on the mechanism of interaction of the passivating TGA ligand with the QDs interface [22–24]. Along with the probability of photolysis of Ag₂S nanocrystals, an assumption has been made about the possible photodesorption of passivator molecules (TGA), as well as their photodestruction.

IR spectra of the surface environment of Ag₂S QDs and core/shell structures based on them

As already noted, the analysis of data demonstrating the effects of exciting radiation on Ag₂S QDs ensembles showed that the photostability of luminescence is determined mainly by the state of the interface of Ag₂S nanocrystals. The role of the ligand in this process can be elucidated using FTIR absorption spectra. To detail the changes in the state of the AgS QDs interfaces, FTIR absorption spectra were studied before and after exposure to exciting radiation leading to degradation of IR luminescence (Fig. 5 and 6).

First of all, the mechanisms of interaction of passivating molecules of TGA and L-Cys ligands with the surface of Ag₂S nanocrystals were established by FTIR spectra. In each of the analyzed FTIR spectra of these samples, the disappearance of the peak corresponding to the stretching vibrations of the S−H-group of TGA and L-Cys molecules ($2559\ \text{cm}^{-1}$) was noted, indicating the attachment of the ligand molecule by the thiol terminal group to the Ag₂S QDs interface (Figures 5 and 6, curves *2*) [22,24,49–51]. The passivation of Ag₂S QDs with TGA and L-Cys molecules leads to the appearance of peaks of asymmetric and symmetric stretching vibrations of the carboxyl group

in the FTIR spectra ($\nu^{\text{as}}(\text{COO}^-)-1567\ \text{cm}^{-1}$ for TGA, $1581\ \text{cm}^{-1}$ for L-Cys; $\nu^{\text{s}}(\text{COO}^-)$ — $1388\ \text{cm}^{-1}$ for TGA, $1399\ \text{cm}^{-1}$ for L-Cys). These patterns indicate the adsorption of passivator molecules on the surface of the Ag₂S QDs with a free carboxyl end group COO^- (Fig. 5, Fig. 6, curves *2*) [22,24,49–51]. In the case of Ag₂S/L-Cys QDs, passivation of QDs interfaces by L-Cys molecules is carried out not only by means of the S−H-group, but also by covalent binding of the NH-group of the passivator with broken bonds on the surface of nanocrystals. Despite the fact that the stretching vibrations of the -NH₂ group are hidden by the presence of stretching vibrations of the bound OH-groups (the region of $3500-3300\ \text{cm}^{-1}$), a decrease in intensity and high-frequency displacement of the out-of-plane vibrations of the -NH₂ group were found ($879\ \text{cm}^{-1}$ and $855\ \text{cm}^{-1}$ to $911\ \text{cm}^{-1}$ and $865\ \text{cm}^{-1}$, respectively), as well as low-frequency displacement of the bending vibration band -NH (from 1510 to $1460\ \text{cm}^{-1}$) of the L-Cys molecule, indicating its interaction with the surface of nanocrystals through amino groups (Fig. 6, curve *2*) [52]. In the case of Ag₂S/TGA QDs and Ag₂S/L-Cys QDs, this type of passivation determines the recombination character of IR luminescence (Fig. 5, curve *2*) [22,24].

For Ag₂S/TGA QDs, with excitonic luminescence is characterized by a low-frequency shift of the peak of symmetric stretching vibrations of the COO^- group from 1388 to $1359\ \text{cm}^{-1}$ with a simultaneous high-frequency shift of the peak of asymmetric valence oscillations of the COO^- from 1567 to $1579\ \text{cm}^{-1}$. This feature indicates the participation of COO^- groups in intermolecular interactions, for example, with Ag₂S QDs interfaces (Fig. 5, curve *3*) [22,24]. In addition, a change in the ratio of the intensities of asymmetric and symmetric stretching vibrations of COO^- was noted (Fig. 5, curve *3*). This feature is associated with a change in the symmetry of vibrations of TGA molecules during their adsorption by carboxyl groups on
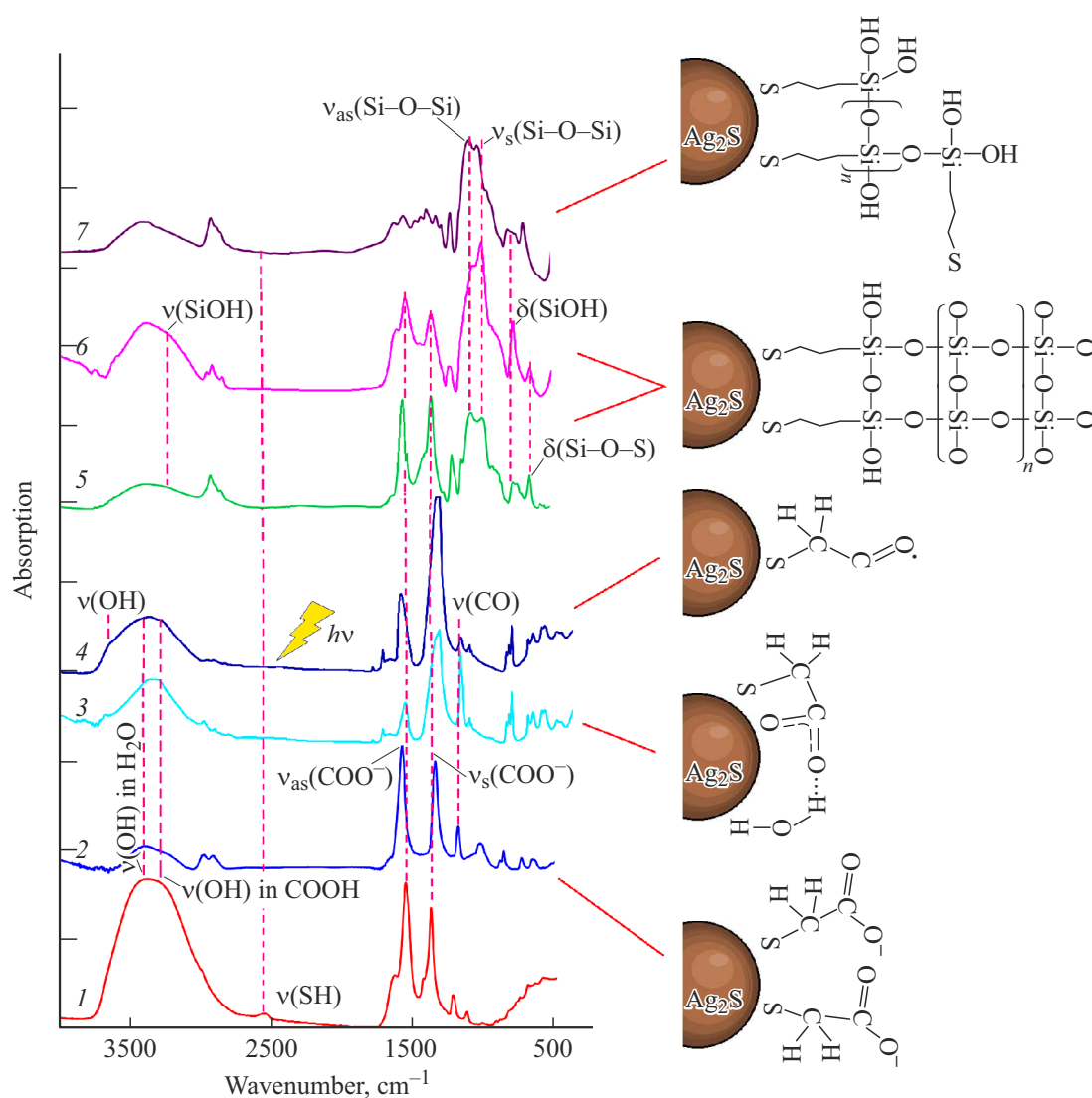
Figure 5. FTIR absorption spectra of TGA (pH 10) —*1*; Ag$_2$S/TGA QDs with trap-state luminescence in the region of $870 - 1000$ nm (before and after exposure) — *2*; Ag$_2$S/TGA QDs with exciton luminescence at 620 nm (up to exposure) — *3*; Ag$_2$S/TGA QDs with exciton luminescence at 620 nm (after exposure) — *4*; Ag$_2$S(TGA)/MPTMS QDs (before and after exposure) — *5*; Ag$_2$S(TGA)/SiO$_2$ QDs (before and after exposure) — *6*; Ag$_2$S/SiO$_2$ QDs (before and after exposure) *7*.

a solid substrate and is characteristic of the formation of carboxylate complexes with broken Ag$_2$S QDs bonds [51].

Thus, different configurations of Ag$_2$S QDs interfaces were characteristic for different types of ligands and passivation conditions with one ligand.

The effect of exciting radiation on Ag$_2$S/TGA QDs obtained by adsorption of thiol groups does not lead to visible changes in the FTIR absorption spectrum (Fig. 5, curve *2*) against the background of photodegradation of luminescence intensity of about 80% (Fig. 4, *a*, curve *1*). Thus, the process of photodestruction of the TGA molecule at its given configuration is not observed at the QDs interface. Only photodesorption of TGA is likely. On the contrary, the effect of exciting radiation on Ag$_2$S/TGA QDs, obtained by adsorption of thiol and carboxyl groups

simultaneously leads to photodegradation of luminescence intensity (Fig. 4, *a*, curve *2*), accompanied by a change in FTIR absorption spectrum (Fig. 5, curves *3, 4*). After exposure, a peak of about 3600 cm^{-1} occurs in the FTIR absorption spectrum, due to vibrations of free or weakly bound OH groups, as well as a significant decrease in intensity in the band of stretching vibrations of CO-groups at 1222 cm^{-1} (Fig. 5, curve *4*). The observed changes are a consequence of a change in the nature of the interaction of TGA molecules with the Ag$_2$S QDs interface as a result of photodestruction of TGA, apparently with the formation of a α-thiol-substituted acyl radical (S$-$CH$_2-$CO$^\bullet$) [22,24,53]. In the case of Ag$_2$S/L-Cys QDs obtained by adsorption of two functional groups simultaneously (thiol and amino groups), the effect of exciting radiation practically does not
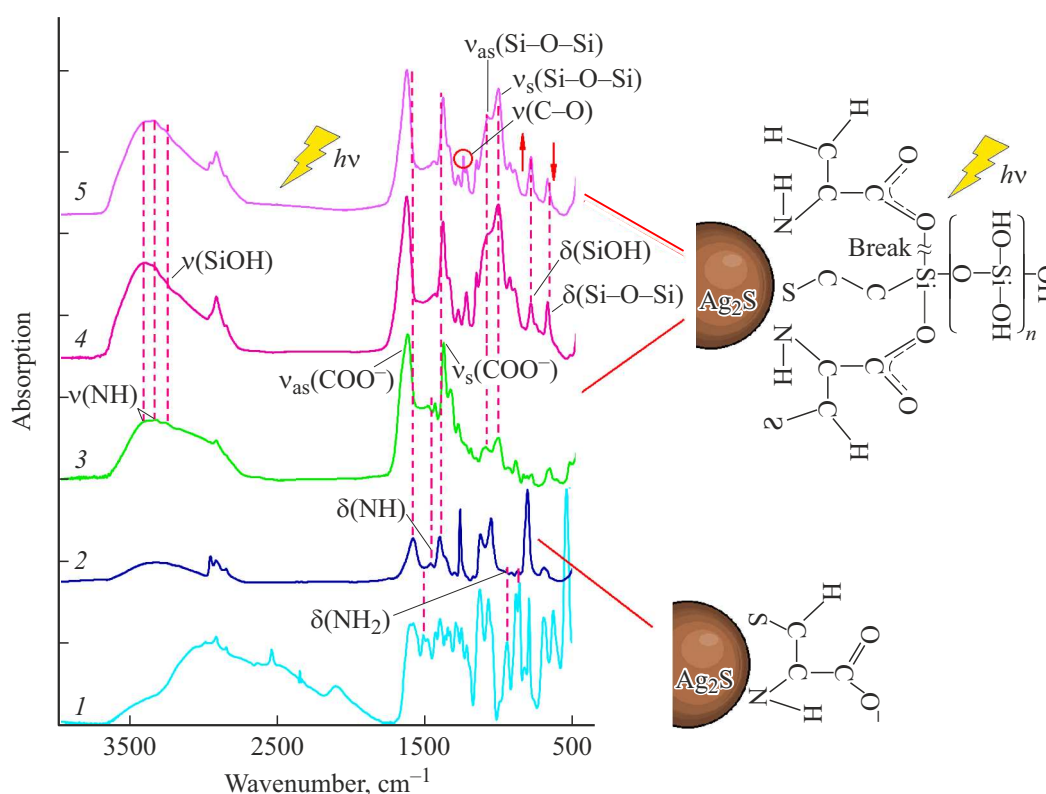
Figure 6. FTIR absorption spectra of L-Cys (pH 10) — *1*; Ag$_2$S/L-Cys QDs (before and after exposure) — *2*; Ag$_2$S(L-Cys)/MPTMS QDs (before exposure) — *3*; Ag$_2$S(L-Cys)/Sao$_2$ QDs (before exposure) — *4*; Ag$_2$S(L-Cys)/SiO$_2$ QDs (after exposure) — *5*.

lead to a loss of their luminescence intensity (Fig. 4, *b*, curve *1*). At the same time, no changes were detected in the FTIR absorption spectrum either (Fig. 6, curve *2*).

The formation of core/shell structures based on Ag$_2$S/TGA QDs and Ag$_2$S/L-Cys QDs leads to a significant transformation of the FTIR spectra (Fig. 5, curves *5* and *6*, fig. 6, curves *3* and *4*). There is a change in the structure and intensity of the characteristic frequency bands of the TGA and L-Cys passivator molecules that determine the structure of the QDs interfaces.

In the case of Ag$_2$S(TGA)/MPTMS QDs, the intensity of the characteristic frequencies of the carboxylate group TGA (COO$^-$) decreases. In this case, there is no spectral shift of the bands ν^{as}(COO$^-$) and ν^s(COO$^-$) relative to their position for an interaction-free acid molecule, which indicates the transition of TGA molecules to a state free from interaction with Ag$_2$S nanocrystals (Fig. 5, curves *5* and *6*). These data confirm the presence in the Ag$_2$S(TGA)/MPTMS QDs system of the ligand replacement process at the QDs interface (ligand exchange) during the formation of the SiO$_2$ layer, when a more reactive MPTMS molecule replaces the TGA [38]. Absence of a peak in the vibration region of the S−H-group (2560 cm^{-1}) for Ag$_2$S(TGA)/MPTMS QDs and Ag$_2$S(L-Cys)/MPTMS QDs indicates that the hydrolyzed form of MPTMS also interacts with the surface of the Ag$_2$S nanocrystal by means of a thiol group (Fig. 5, curves *5* and *6*, Fig. 6, curves *3* and *4*).

However, in the case of Ag$_2$S(L-Cys)/MPTMS QDs, the L-Cys passivator molecules remain on the surface of nanocrystals due to interaction with the amino group, which confirms the presence of ν(NH) stretching bands in the IR spectrum in the region of 3200−3300 cm^{-1} and bending vibrations δ(NH) in the region of 1460 cm^{-1}, characteristic of adsorbed NH$_2$-groups (Fig. 6, curves *3* and *4*). At the same time, the frequency shift of asymmetric and symmetric stretching vibrations of the COO$^-$ group from 1581 to 1588 cm^{-1} and from 1399 to 1386 cm^{-1} may probably indicate the involvement of the carboxylate aninone of the L-Cys molecule in a weak interaction with silicon and water atoms. These patterns indicate the formation of a fragmentary shell of SiO$_2$/L-Cys on the surface of Ag$_2$S/L-Cys QDs.

As a result of the formation of Ag$_2$S(TGA)/MPTMS QDs and Ag$_2$S(L-Cys)/MPTMS QDs the FTIR spectrum, peaks also occur with frequencies corresponding to the vibrations of siloxane (1103 cm^{-1} (ν_{as}(Si−O−Si)), 1023 cm^{-1} (ν_s(Si−O−Si) and 800 cm^{-1}δ(Si-O-Si)) and silanol groups 3260(ν(SiON)) and 928 cm^{-1} (δ(SiON)) (fig. 5, curve *5*, fig. 6, curve *3*). At the same time, the intensity of the band of asymmetric vibrations of the siloxane group (ν_{as}(Si−O−Si) = 1103 cm^{-1}) exceeds the intensity of the band of symmetric stretching vibrations (ν_s(Si−O−Si) = 1023 cm^{-1}). For the model sample of Ag$_2$S/SiO$_2$ QDs, in which the silica ligand MPTMS si-

multaneously served as both a passivating ligand and a precursor of the shell SiO_2, the intensity of the vibration band $\nu_{as}(Si-O-Si)$ also exceeds the intensity of symmetric vibrations $\nu_s(Si-O-Si)$ (Fig. 5, curve 7). This pattern indicates in favor of the formation of cyclic siloxane structures by MPTMS molecules, which form long-chain polymers completed with a sulfogroup, which prevents the growth of the thickness of the SiO shell$_2$ [54,55].

Thus, for QDs of $Ag_2S(TGA)/MPTMS$, $Ag_2S(L-Cys)/MPTMS$ and Ag_2S/SiO_2 is characteristic formation of a thin SiO_2 shell ($\sim 1-2$ monolayers) due to the structural features of MPTMS molecules, which is consistent with the analysis of TEM images. An increase in the thickness of the SiO_2 shell at the QDs interfaces when Na_2SiO_3 is introduced demonstrates a redistribution of intensity in the bands of stretching vibrations of the silaxane group (Fig. 5, curves 6, Fig. 6, curves 4). This feature may be related to the elongation of $Si-O-Si$ chains on the surface of QDs [54].

For QDs samples of $Ag_2S(L-Cys)/MPTMS$ and $Ag_2S(L-Cys)/SiO_2$ showing a significant decrease in the intensity of the luminescence under the action of exciting radiation (Fig. 4, b), in the FTIR absorption spectra against the background of bands in the region of $1230-1260\,cm^{-1}$, there is the appearance of another more intense band with a peak of $1260\,cm^{-1}$, which corresponds to stretching oscillations with $-O$-groups [22,24], as well as the redistribution of the intensity of the bands of $\delta(SiON)$ and $\delta(Si-O-Si)$ groups in the region of $660-950\,cm^{-1}$. This fact may indicate the destruction of the fragmentary shell $(L-Cys)/SiO_2$ under the action of exciting radiation by „breaking" $Si-O-C$-bond (Fig. 6, curve 5). For QDs of $Ag_2S(TGA)/MPTMS$, $Ag_2S(TGA)/SiO_2$ and Ag_2S/SiO_2, demonstrating the stability of the luminescence intensity to the effect of exciting radiation, there are no changes in the FTIR spectra.

Discussion of results

The empirical results obtained indicate the influence of the ligand type and its coordination on the photostability of the luminescent properties of Ag_2S QDs. Thus, for Ag_2S/TGA QDs, the analysis of FTIR absorption spectra indicates two possible mechanisms of binding of TGA molecules to the QDs interface.

The first mechanism is due to the adsorption of thiol groups of TGA molecules at the QDs interface. This passivation mechanism leads to significant photodegradation of IR luminescence of Ag_2S/TGA QDs ($\sim 80\%$). However, in this case, photodegradation of the luminescence of Ag_2S/TGA QDs is reversible. Reversible photodegradation of Ag_2S/TGA QDs is due to the photochemical reaction of the formation of additional channels of nonradiative recombination due to the initial stage of photolysis of QDs interfaces, presumably associated with the transformation of low-atomic silver clusters, which are photo- and thermon-estable [22–24].

The second mechanism is realized, apparently, due to the adsorption of both thiol and carboxyl groups of TGA molecules at the QDs interface. The observed irreversible photodegradation of luminescence Ag_2S/TGA QDs, according to FTIR absorption spectra, is caused by a change in the nature of the interaction of TGA molecules with the Ag_2S QDs interface as a result of photodestruction of TGA with the formation of the radical $S-CH_2-CO^\bullet$ [22,24].

For $Ag_2S/L-Cys$ QDs, the interaction of L-Cys with the QDs surface by means of two functional groups simultaneously (thiol and amino groups) is also shown. However, this mechanism of passivation of Ag_2S QDs, ensures the stability of luminescence of $Ag_2S/L-Cys$ QDs under prolonged exposure to exciting radiation, apparently due to the elimination of broken bonds at the interfaces of QDs and, as a consequence, localization of charge carriers in the volume of QDs. No changes in the FTIR absorption spectra of L-Cys interface molecules were detected for $Ag_2S/L-Cys$ QDs.

The FTIR absorption spectra of the studied core/shell QDs samples showed that the structure of the SiO_2 shell strongly depends on the type of Ag_2S QDs passivator molecules used. At the same time, the shell structure established by FTIR spectroscopy correlates with the data on photodegradation of luminescence. Thus, the addition of MPTMS to Ag_2S/TGA QDs, provides an effective replacement of TGA interface molecules with MPTMS, which ensures an increase in quantum yield and blocking photodegradation of Ag_2S/TGA QDs luminescence. Further growth of the SiO shell$_2$ (of Na_2SiO_3) does not change its structure and also provides high luminescence stability. An increase in the stability of FTIR luminescence of $Ag_2S(TGA)/MPTMS$ QDs, and $Ag_2S(TGA)/SiO_2$ QDs is in agreement with data on a decrease in the efficiency of nonradiative recombination in the formation of core/shell structures (table). This feature also indicates that in Ag_2S/TGA QDs, the process of degradation of IR luminescence under the action of exciting radiation is due to the photochemical reaction of the formation of additional channels of non-radiative recombination.

On the contrary, for $Ag_2S/L-Cys$ QDs, initially possessing photostable luminescence, the introduction of MPTMS leads to significant degradation of luminescence under the action of exciting radiation. According to IR spectroscopy data, the formation of $Ag_2S(L-Cys)/MPTMS$ QDs is accompanied by partial passivator replacement, while MPTMS and L-Cys molecules are present at the interface simultaneously. The effect of exciting radiation on $Ag_2S(L-Cys)/MPTMS$ QDs, and $Ag_2S(L-Cys)/SiO_2$ QDs leads to irreversible degradation of luminescence intensity due to photodestruction of the fragmentary $(L-Cys)/SiO_2$ shell, leading to the formation of nonradiative recombination channels. In favor of increasing the efficiency of nonradiative recombination as exciting radiation is exposed to QDs of $Ag_2S(L-Cys)/MPTMS$ and $Ag_2S(L-Cys)/SiO_2$, it also indicates an increase in the

constant of nonradiative recombination and a reduction in the lifetime of luminescence (table).

Conclusion

The analysis of the obtained results indicates a significant influence of the state of the interfaces on the stability of the Ag$_2$S QDs luminescence, and the core/shell structures based on them. According to FTIR spectroscopy data, the structure of the SiO$_2$ shell determines the photostability of the luminescence of Ag$_2$S QDs. It is shown that the formation of the SiO$_2$ shell by replacing the passivating TGA ligand with MPTMS on the surface of the Ag$_2$S QDs ensures the stability of luminescence under prolonged exposure to exciting radiation. At the same time, the partial replacement of the passivating ligand L-Cys, due to its initial mechanism of interaction with the Ag$_2$S QDs interface, ensures the formation of a fragmentary shell (L-Cys)/SiO$_2$. At the same time, the effect of exciting radiation on the Ag$_2$S(L-Cys)/SiO$_2$ QDs leads to irreversible photodegradation of the luminescence of the Ag$_2$S QDs, which, according to FTIR spectroscopy data, is the result of photodestruction of the (L-Cys)/SiO$_2$ shell.

Conflict of interest

The authors declare that they have no known financial conflicts of interest or personal relationships that could affect the work presented in this article.

References

[1] M.A. Cotta. ACS Appl. Nano Mater., **3** (6), 4920 (2020). DOI: 10.1021/acsanm.0c01386

[2] S.B. Hafiz, M. Scimeca, A. Sahu, D.-K. Ko. Nano Convergence, **6**, 7 (2019). DOI: 10.1186/s40580-019-0178-1

[3] F. Boschi, F. Sanctis // Eur. J. Histochem., **61** (3), 2830 (2017). DOI: 10.4081/ejh.2017.2830

[4] Ph. Reineck, M. Torelli. Material Matters, **14** (2), 57 (2019).

[5] V. Caponetti, J.W. Trzcinski, A. Cantelli, R. Tavano, E. Papini, F. Mancin, M. Montalti. Front. Chem., **7**, 168 (2019). DOI: 10.3389/fchem.2019.00168

[6] O.S. Wolfbeis. Chem. Soc. Rev., **44**, 4743 (2015). DOI: 10.1039/C4CS00392F

[7] A.P. Litvin, I.V. Martynenko, F. Purcell-Milton, A.V. Baranov, A.V. Fedorov, Y.K. Gun'ko. J. Mater. Chem. A, **5**, 13252 (2017). DOI: 10.1039/C7TA02076G

[8] Z. Wang, N. Zhang, L. Kimber, K.L. Brenneman, T.-C. Wu, H.-C. Jung, S. Biswas, B. Sen, K. Reinhardt, S. Liao, M. Stroscio, M. Dutta. *Quantum Dot Devices, 1st ed* (Springer New York, NY, 2012). DOI: 10.1007/978-1-4614-3570-9_15

[9] M. Chen, L. Lu, H. Yu, C. Li, N. Zhao. Advanced Science, **8** (18), 182101560 (2021). DOI: 10.1002/advs.202101560

[10] L. Colace, A. Iacovo, C. Venettacci. Colloidal quantum dots for optoelectronic applications: Fundamentals and recent progress. In: *20th Italian National Conference on Photonic Technologies* (Fotonica 2018) (IET, 2018), p. 1. DOI: 10.1049/cp.2018.1626

[11] Y. Miao, P. Yang, J. Zhao, Y. Du, H. He, Y. Liu. J. Nanoscience and Nanotechnology, **15** (6), 4462-9 (2015). DOI: 10.1166/jnn.2015.9800

[12] A.S. Tsipotan, M.A. Gerasimova, S.P. Polyutov, A.S. Aleksandrovsky, V.V. Slabko. J. Phys. Chem. B, **121** (23), 5876 (2017). DOI: 10.1021/acs.jpcb.7b03166

[13] A. Kumari, R.R. Singh. Physica E: Low-dimensional Systems and Nanostructures, **89**, 77 (2017). DOI: 10.1016/j.physe.2017.01.031

[14] Q.F. Ma, J.Y. Chen, P.N. Wang, Y. Yue, N. Dai. J. Lumin., **131** (1), 2267 (2011). DOI: 10.1016/j.jlumin.2011.05.055

[15] J. Ma, J.Y. Chen, Y. Zhang, P.N. Wang, J. Guo, W.-L. Yang, C.-C. Wang. J. Phys. Chem. B, **111** (41), 12012 (2007). DOI: 10.1021/jp073351+

[16] T. Wang, X. Jiang. ACS Appl. Mater. Interfaces, **5** (4), 1190 (2013). DOI: 10.1021/am302234z

[17] M. Bhati, S.A. Ivanov, T.P. Senftle, S. Tretiak, D. Ghosh. J. Mater. Chem. A, **10**, 5212 (2022). DOI: 10.1039/D1TA07983B

[18] H.H.-Y. Wei, C.M. Evans, B.D. Swartz, A.J. Neukirch, J. Young, O.V. Prezhdo, T.D. Krauss. Nano Lett., **12**, 4465 (2012). DOI: 10.1021/nl3012962

[19] A. Kurzmann, A. Ludwig, A.D. Wieck, A. Lorke, M. Geller. Nano Lett., **16**, 3367 (2016). DOI: 10.1021/acs.nanolett.6b01082

[20] Y. Zeng, D.F. Kelley. ACS Nano, **9** (10), 10471 (2015). DOI: 10.1021/acsnano.5b04710

[21] M.S. Smirnov, O.V. Ovchinnikov, I.G. Grevtseva, A.I. Zvyagin, A.S. Perepelitsa, R.A. Ganeev. Opt. Spectrosc., **124** (5), 681 (2018). DOI: 10.1134/S0030400X18050211

[22] O.V. Ovchinnikov, I.G. Grevtseva, M.S. Smirnov, T.S. Kondratenko, A.S. Perepelitsa, S.V. Aslanov, V.U. Khokhlov, E.P. Tatyanina, A.S. Matsukovich. Optical and Quantum Electronics, **52** (4), 198 (2020). DOI: 10.1007/s11082-020-02314-8

[23] O.V. Ovchinnikov, I.G. Grevtseva, M.S. Smirnov, T.S. Kondratenko. J. Lumin., **207**, 626 (2019). DOI: 10.1016/j.jlumin.2018.12.019

[24] T. Kondratenko, O. Ovchinnikov, I. Grevtseva, M. Smirnov, O. Erina, V. Khokhlov, B. Darinsky, E. Tatianina. Materials, **13** (4), 909 (2020). DOI: 10.3390/ma13040909

[25] I.G. Grevtseva, S.V. Aslanov. Bulletin of the Russian Academy of Sciences: Physics, **84** (5), 517 (2020). DOI: 10.3103/s1062873820050111

[26] O.V. Ovchinnikov, T.S. Kondratenko, I.G. Grevtseva, M.S. Smirnov, S.I. Pokutnyi. J. Nanophotonics, **10** (3), 033505 (2016). DOI: 10.1117/1.JNP.10.033505

[27] O.V. Ovchinnikov, M.S. Smirnov, T.S. Kondratenko, S.A. Ambrosevich, M.T. Metlin, I.G. Grevtseva, A.S. Perepelitsa. J. Nanoparticle Research, **19** (12), 403 (2017). DOI: 10.1007/s11051-017-4093-2

[28] O.V. Ovchinnikov, A.S. Perepelitsa, M.S. Smirnov, A.N. Latyshev, I.G. Grevtseva, G.N. Goltsman, R.B. Vasiliev, A.G. Vitukhnovsky. J. Lumin., **220**, 117008 (2020). DOI: 10.1016/j.jlumin.2019.117008

[29] V.A. Krivenkov, P.S. Samokhvalov, P.A. Linkov, D.O. Solovyeva, G.E. Kotkovskii, A.A. Chistyakov, I. Nabiev. In: *Proceedings Volume 9126, Nanophotonics V*, 91263N (2014). DOI: 10.1117/12.2057828

[30] D.L. Nida, N. Nitin, W.W. Yu, V. L. Colvin, R. Richards-Kortum. Nanotechnology, **19** (3), 035701 (2008). DOI: 10.1088/0957-4484/19/03/035701

[31] Y. Sun, F. Song, C. Qian, K. Peng, S. Sun, Y. Zhao, Z. Bai, J. Tang, S. Wu, H. Ali, F. Bo, H. Zhong, K. Jin, X. Xu. ACS Photonics, **4**, 369 (2017). DOI: 10.1021/acsphotonics.6b00843

[32] E.V. Klyachkovskaya, S.V. Vashchenko, A.P. Stupak, S.V. Gaponenko. J. Appl. Spectrosc., **77**, 793 (2010). DOI: 10.1007/s10812-010-9395-4

[33] K.V. Vokhmintcev, C. Guhrenz, N. Gaponik, I. Nabiev, P.S. Samokhvalov. J. Phys. Conf. Ser., **784**, 012014 (2017). DOI: 10.1088/1742-6596/784/1/012014

[34] D. Vasudevan, R.R. Gaddam, A. Trinchi, I. Cole. J. Alloys and Compounds, **636**, 395 (2015). DOI: 10.1016/j.jallcom.2015.02.102

[35] J. Kim, D. Hwang, H. Jung, K. Kim, X.-H. Pham, S.-H. Lee, J. Byun, W. Kim, H.-M. Kim, E. Hahm, K.-m. Ham, W.-Y. Rho, D. Lee, B.-H. Jun. J. Nanobiotechnol., **20**, 22 (2022). DOI: 10.1186/s12951-021-01227-2

[36] M.S. Smirnov, O.V. Buganov, S.A. Tikhomirov, O.V. Ovchinnikov, E.V. Shabunya-Klyachkovskaya, I.G. Grevtseva, T.S. Kondratenko. J. Nanoparticle Research, **19**, 376 (2017). DOI: 10.1007/s11051-017-4067-4

[37] K.D. Wegner, F. Dussert, D. Truffier-Boutry, A. Benayad, D. Beal, L. Mattera, W.L. Ling, M. Carriére, P. Reiss. Front. Chem., **27** (7), 466 (2019). DOI: 10.3389/fchem.2019.00466

[38] A.S. Perepelitsa, O.V. Ovchinnikov, M.S. Smirnov, T.S. Kondratenko, I.G. Grevtseva, S.V. Aslanov, V.Y. Khokhlov. J. Lumin., **231**, 117805 (2021). DOI: 10.1016/j.jlumin.2020.117805

[39] I. Piwonski, J. Grobelny, M. Cichomski, G. Celichowski, J. Rogowski. Applied Surface Science, **242** (1−2), 147 (2005). DOI: 10.1016/j.apsusc.2004.08.009

[40] Sh. Lin, Y. Feng, X. Wen. Phys. Chem., **119**, 867 (2015). DOI: 10.1021/ jp511054g.

[41] M.S. Smirnov, O.V. Ovchinnikov. J. Lumin., **227**, 117526-1-8 (2020). DOI: 10.1016/j.jlumin.2020.117526

[42] N. Fujimura, A. Ohta, K. Makihara, S. Miyazaki. Jpn. J. Appl. Phys., **55**, 08PC06 (2016). DOI: 10.7567/JJAP.55.08PC06

[43] A.N. Latyshev, O.V. Ovchinnikov, S.S. Okhotnikov. J. Appl. Spectrosc., **70** (6), 817 (2003). DOI: 10.1023/B:JAPS.0000016295.19263.97

[44] V.M. Ievlev, A.N. Latyshev, O.V. Ovchinnikov, M.S. Smirnov, V.G. Klyuev, A.M. Kholkina, A.N. Utekhin, A.B. Evlev. Doklady Physics, **51** (8), 400 (2006). DOI: 10.1134/S1028335806080027

[45] O.V. Ovchinnikov, M.S. Smirnov, A.N. Latyshev, D.I. Stasel'ko. Opt. Spectrosc., **103** (3), 482 (2007).

[46] M.S. Smirnov, O.V. Ovchinnikov, I.G. Grevtseva, A.I. Zvyagin, A.S. Perepelitsa, R.A. Ganeev. Opt. Spectrosc., **124** (5), 681 (2018). DOI: 10.1134/S0030400X18050211

[47] A.N. Latyshev, O.V. Ovchinnikov, V.G. Klyuev, M.S. Smirnov, D.I. Stasel'ko. Opt. Spectrosc., **114** (4), 544 (2013). DOI: 10.1134/S0030400X13040115

[48] M.S. Smirnov, O.V. Ovchinnikov, N.A.R. Hazal, A.I. Zvyagin. Inorganic Materials, **54** (5), 413 (2018). DOI: 10.1134/S002016851805014X

[49] Z.T. Banizi, M. Seif. Mater. Res. Express, **4** (10), 105007 (2017). DOI: 10.1088/2053-1591/aa8a8a

[50] F.O. Silva, M.S. Carvalho, R. Mendoną, W.A.A. Macedo, K. Balzuweit, P. Reiss, M.A. Schiavon. Nanoscale Res. Lett., **7** (1), 536 (2012). DOI: 10.1186/1556-276X-7-536

[51] Ch. Chung, M. Lee. Bull. Korean Chem. Soc., **25** (10), 1461 (2004). DOI: 10.5012/bkcs.2004.25.10.1461

[52] K. Nakamoto. *IR spectra and Raman spectra of inorganic and coordination compounds* (Mir, Moscow, 1991).

[53] A.R. Attar, D.E. Blumling, K.L. Knappenberger. J. Chem. Phys., **134**, 024514 (2011). DOI: 10.1063/1.3526746

[54] M.-A. Chen, X.-B. Lu, Z.-H. Guo, R. Huang. Corrosion Science, **53** (9), 2793 (2011). DOI: 10.1016/j.corsci.2011.05.010

[55] N. Nuryono, N.M. Rosiati, B. Rusdiarso, S.C.W. Sakti, S. Tanaka. Springerplus, **11** (3), 515 (2011). DOI: 10.1186/2193-1801-3-515